Finite Element Analysis Comparing the Biomechanical Parameters in Multilevel Posterior Cervical Instrumentation Model Involving Lateral Mass Screw versus Transpedicular Screw Fixation at the C7 Vertebra

Arvind Gopalrao Kulkarni[1], Priyambada Kumar[2], Gautam Manjayya Shetty[3,4],
Sandipan Roy[5], Pechimuthu Susai Manickam[5], Raja Dhason[5],
Aditya Raghavendra Sai Siva Chadalavada[2], Yogesh Madhavrao Adbalwad[2]

[1]Department of Spine Surgery, Mumbai Spine Scoliosis and Disc Replacement Centre, Mumbai, India
[2]Department of Spine Surgery, Bombay Hospital and Medical Research Centre, Mumbai, India
[3]Department of Orthopaedic Surgery, Knee & Orthopedic Clinic, Mumbai, India
[4]Department of Clinical Research, AIMD Research, Mumbai, India
[5]Department of Mechanical Engineering, SRM Institute of Science and Technology, Kattankulathur, India

Study Design: Basic research.

Purpose: This finite element (FE) analysis (FEA) aimed to compare the biomechanical parameters in multilevel posterior cervical fixation with the C7 vertebra instrumented by two techniques: lateral mass screw (LMS) vs. transpedicular screw (TPS).

Overview of Literature: Very few studies have compared the biomechanics of different multilevel posterior cervical fixation constructs.

Methods: Four FE models of multilevel posterior cervical fixation were created and tested by FEA in various permutations and combinations. Generic differences in fixation were determined, and the following parameters were assessed: (1) maximum moment at failure, (2) maximum angulation at failure, (3) maximum stress at failure, (4) point of failure, (5) intervertebral disc stress, and (6) influence of adding a C2 pars screw to the multilevel construct.

Results: The maximum moment at failure was higher in the LMS fixation group than in the TPS group. The maximum angulation in flexion allowed by LMS was higher than that by TPS. The maximum strain at failure was higher in the LMS group than in the TPS group. The maximum stress endured before failure was higher in the TPS group than in the LMS group. Intervertebral stress levels at C6–C7 and C7–T1 intervertebral discs were higher in the LMS group than in the TPS group. For both models where C2 fixation was performed, lower von Mises stress was recorded at the C2–C3 intervertebral disc level.

Conclusions: Ending a multilevel posterior cervical fixation construct with TPS fixation rather than LMS fixation at the C7 vertebra provides a stiff and more constrained construct system, with higher stress endurance to compressive force. The constraint and durability of the construct can be further enhanced by adding a C2 pars screw in the fixation system.

Keywords: Finite element analysis; Transpedicular screw fixation; Lateral mass screw fixation; Posterior cervical fixation; Intervertebral disc stress

Introduction

Posterior cervical spine stabilization and fusion is frequently performed to address various cervical pathologies [1]. In long cervical fixation constructs, the necessity of establishing a secure anchor at the C7 vertebra cannot be underestimated [2]. Current posterior subaxial cervical spine stabilization systems primarily employ a screw–rod design [3]. These biomechanically sturdy designs are associated with higher fusion rates, early mobilization, faster rehabilitation, and ultimately better clinical outcomes [4,5]. Although several posterior cervical decompression and fusion procedures are performed annually, dispute persists regarding the most effective surgical approach, particularly with respect to the selection of the upper and lower instrumented levels in a multilevel construct. Most studies to date have focused primarily on the controversies around the technique and level of the lower instrumented body. On the contrary, few studies have analyzed the effect of terminating the construct proximally at the C2 vertebra instead of at C3 [6,7]. Extending the construct proximally to the C2 vertebra allows a tri-column stabilizer effect of the construct. However, this is associated with longer surgical duration, risk of iatrogenic vascular injury, and greater tissue handling [7]. One of the most common anchors used for posterior fixation at the C7 vertebra is the lateral mass screw (LMS) fixation. The most significant benefit is that it offers reliable fixation and has a low rate of neurovascular damage [8-10]. Cervical pedicle screw fixation, although precarious and challenging from C3 to C6 [11], is practically possible at the C7 vertebra because of its homology to the thoracic vertebrae and favorable relationship with the vertebral artery [12]. Furthermore, because the C7 vertebra is frequently the most caudal point of fixation in multilevel structures and the location of greatest stress concentration, concerns about appropriate screw placement are frequently centered on the C7 vertebra [13]. As regards multilevel posterior cervical fixation construct, groups have polar views: one advocating LMS at the C7 vertebra caudally primarily because of technical ease and relatively lower incidence of vascular and neurologic injury, and the other favoring transpedicular screws (TPS) at the C7 vertebra because of the higher pullout strength of the screw [13]. Over the years, studies have discussed the advantages and drawbacks of LMS and TPS at the C7 vertebra caudally, along with the preference for various fixation techniques based on patient demographics [12-15]. However, studies comparing the biomechanics of different multilevel posterior cervical fixation constructs are limited. In this finite element (FE) analysis (FEA), we aimed to compare the biomechanical parameters of commonly utilized multilevel posterior cervical fixation constructs incorporating the C7 vertebra using two techniques: LMS fixation versus TPS fixation. This FEA study can be a reference for further research and clinical adaptation in the field.

Materials and Methods

1. Generation and validation of the finite element model

Computed tomography (CT) scan of a healthy 35-year-old man was used to construct a three-dimensional (3D) FE model of a typical cervical segment ranging from the skull base to the T1 vertebra [16,17] (Fig. 1). Mimics ver. 10.01 (Materialise, Leuven, Belgium) was used for importing the scans and recreating the vertebra levels. The geometric model was then transferred to Geomagic Design ver. X16.0 (Geomagic, Durham, NC, USA) for refining procedure. Using HyperMesh software (Altair Engineering, Troy, MI, USA), the intervertebral disc, ligaments, and vertebral bone meshing were created and loaded into ANSYS ver. 18.2. software (ANSYS Inc., Southfield, MI, USA). ANSYS was utilized to define the element type, material property, and loading condition. The C2–T1 cervical vertebral bodies, posterior bony elements, intervertebral disc consisting of the annulus fibrosus and nucleus pulposus, inferior and superior vertebral endplates, and ligaments were all incorporated in the cervical spine FE model. The literature-recommended intervertebral disc height was maintained [18-22]. The vertebrae, discs, and endplates were all assigned the element property of first-order solid tetrahedral elements.

The model assessed the anterior longitudinal ligament, capsular ligament, posterior longitudinal ligament, interspinous ligament, and ligamentum flavum [18-22]. The ligaments' geometry was recreated using literature data [18-23]. Two-node tension link elements were used to simulate these ligaments. The material properties of the FE model are presented in Table 1 [23-26]. After performing the convergence test, the ideal size for the tetrahedral element was determined to be 0.5 mm [24]. For our FE model, the convergence test's accuracy was 3% [27]. At the superior endplate of the C2 vertebra, a preload of 50
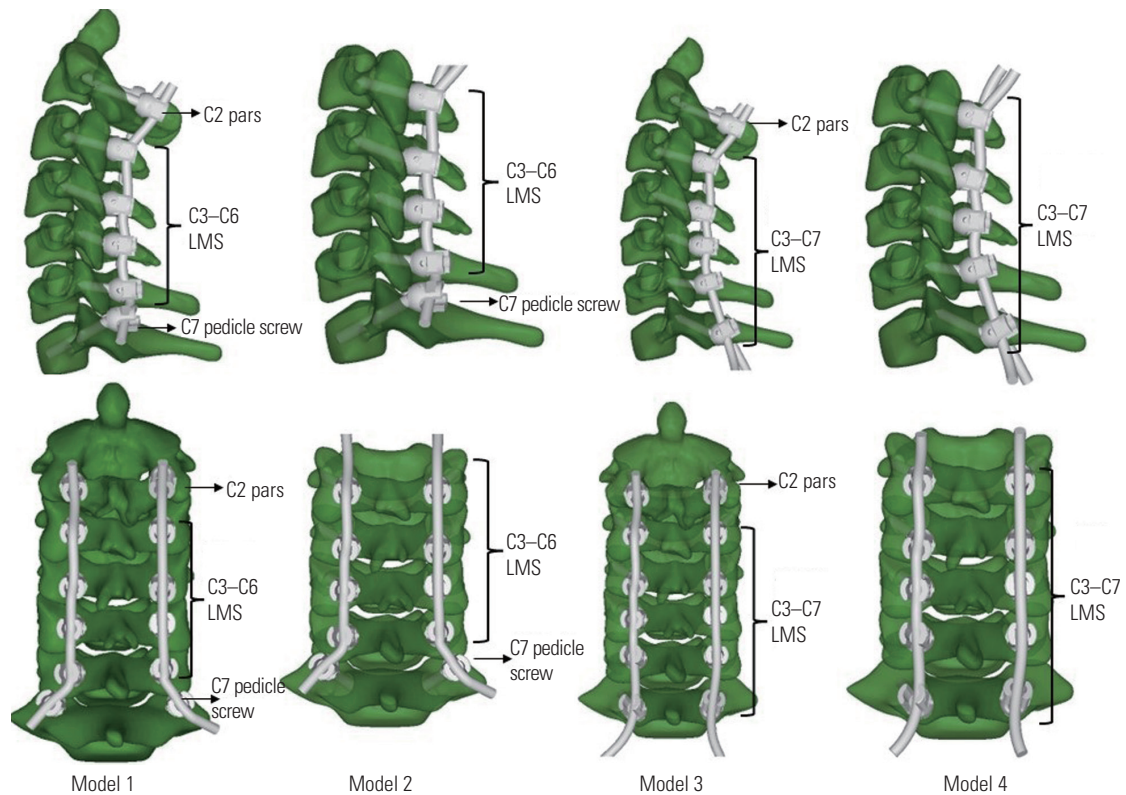
Fig. 1. Three-dimensional surface model of cervical spine with posterior side screw implant for all the constructs. Model 1 shows C2–C7 level with C2 pars C3–C6 lateral mass screw (LMS) and C7 trans-pedicular screw (TPS). Model 2 shows C3–C7 level with C3–C6 LMS and C7 TPS. Model 3 shows C2–C7 level with C2 pars with C3–C7 LMS. Model 4 shows C2–C7 level with C2 pars and C3–C7 LMS. Model 5 shows C3–C7 level with C3–C7 LMS.

Table 1. Materials and properties of cervical spine construct

Component	Element type	Young's modulus (MPa)	Poisson's ratio	Cross-sectional area (mm²)	References
Bony structures					
Vertebral cortical bone	Solid	12,000.0	0.29		[25]
Vertebral cancellous bone	Solid	450.0	0.29		[25]
Posterior bone	Solid	3,500.0	0.29		[25]
End plate	Solid	500.0	0.40		[25]
Intervertebral disc					
Annulus fibrosus	Solid	3.4	0.40		[25]
Nucleus pulposus	Solid	1.0	0.49		[25]
Ligaments					
Anterior longitudinal ligament	Link (tension only)	30.0		6	[25,26]
Posterior longitudinal ligament	Link (tension only)	20.0		5	[25,26]
Interspinous ligament	Link (tension only)	1.5		10	[25,26]
Ligamentum flavum	Link (tension only)	1.5		10	[25,26]
Capsular ligament	Link (tension only)	20.0		5	[25,26]
Implant					
Pedicle screw and rod	Solid	110,000	0.3		[27]

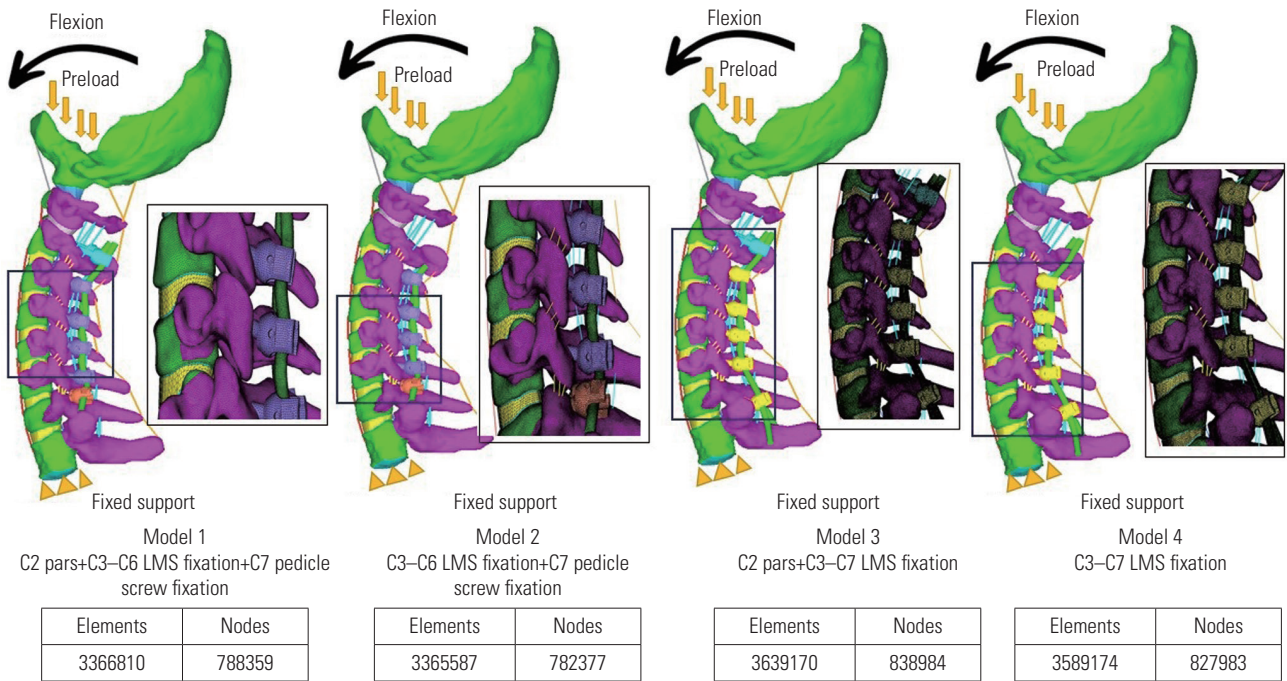CoF (bone-titanium interface)=0.3. Failure of the titanium yield point=900.

Fig. 2. Three-dimensional finite element model of cervical spine C0 to T1 level with boundary condition. Model 1 shows C2–C7 level with C2 pars C3–C6 lateral mass screw (LMS) and C7 trans-pedicular screw (TPS). Model 2 shows C3–C7 level with C3–C6 LMS and C7 TPS. Model 3 shows C2–C7 level with C2 pars with C3–C7 LMS. Model 4 shows C2–C7 level with C2 pars and C3–C7 LMS. Model 5 shows C3–C7 level with C3–C7 LMS.
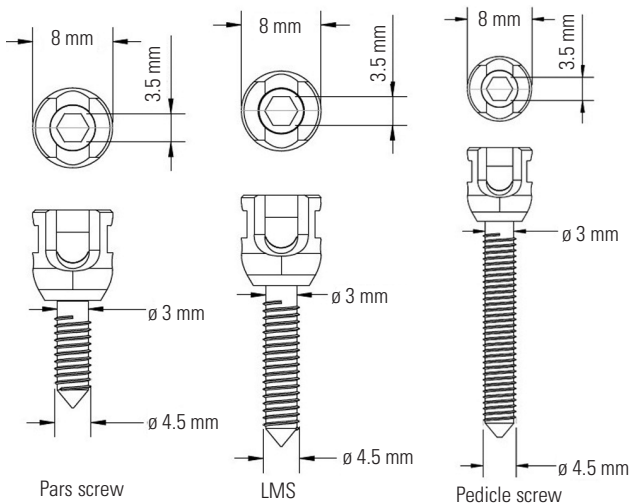

Fig. 3. Geometry of the pars, lateral mass screw (LMS), and trans-pedicular screw (TPS) screws with dimensions.

N of compressive force was applied to replicate the head weight, along with moment variations [16,27]. The inferior endplate of the C7 level motion was fully constrained in each loading protocol (Fig. 2). The dimensions of the screws are provided in Fig. 3.

Four 3D FE models of multilevel posterior cervical fixation ranging from the skull base to the T1 vertebra were tested and compared by FE analysis in various permutations and combinations (Fig. 2): model 1: C2 pars C3–C6 LMS and C7 pedicle screws; model 2: C3–C6 LMS and C7 pedicle screws; model 3: C2 pars and C3–C7 LMS; and model 4: C3–C7 LMS.

In all models, laminectomy was not performed.

Principles of screw fixation and screw trajectory in posterior cervical instrumentation were followed (Fig. 4) [17]: (1) LMS involve only the posterior column from C3 to C7. (2) Pars screws involved only the posterior column at C2. (3) Pedicle screws involved all three columns at C7. (4) LMS were directed laterally and cranially. (5) Pars screws were directed medially and cranially. (6) Pedicle screws were directed medially and neutrally.

2. Material properties and dimensions

The materials were titanium alloy LMS, pedicle screw, pars screws, and connecting rods. The dimensions of screws used were represented in Fig. 3: (1) lateral mass and C2 pars screws: 3.5 mm in diameter and 12–18 mm in length; (2) C7 pedicle screw: 4 mm in diameter and 24–30 mm in length; and (3) T1 pedicle screw: 4 mm in diameter and 30–40 mm in length. The dimensions of the

Model 1   Model 2   Model 3   Model 4
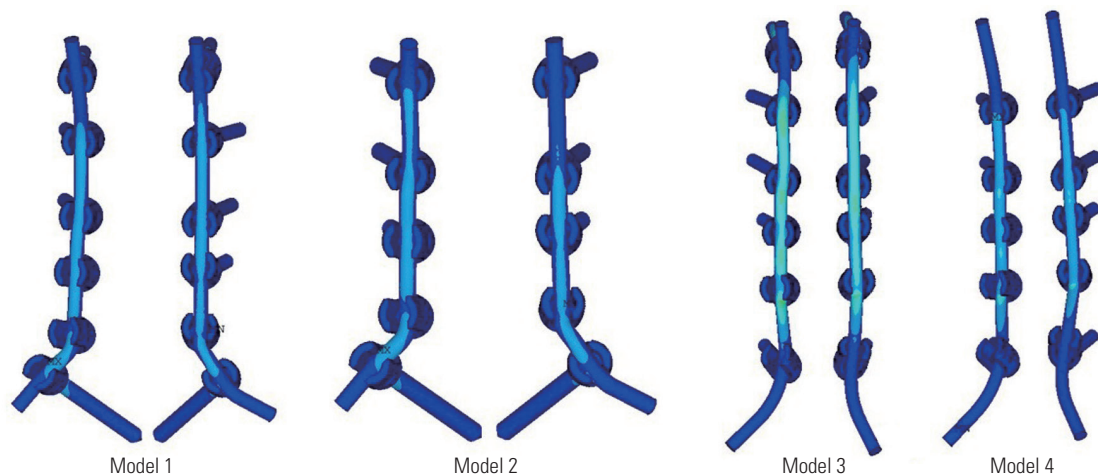
Fig. 4. von Mises stress distribution in the implants. Model 1 shows C2–C7 level with C2 pars C3–C6 lateral mass screw (LMS) and C7 trans-pedicular screw (TPS). Model 2 shows C3–C7 level with C3–C6 LMS and C7 TPS. Model 3 shows C2–C7 level with C2 pars with C3–C7 LMS. Model 4 shows C2–C7 level with C2 pars and C3–C7 LMS.

rods used were 3.2 mm in diameter.

3. Loading conditions

For each model, at the superior endplate of the C2 vertebra, a preload of 50 N of compressive force was applied to replicate the head weight along with moment variations [16,27]. In each loading protocol, the inferior endplate of C7 level motion was fully constrained. The same boundary and loading conditions were adapted for all four models.

4. Parameters to be recorded

The following parameters were recorded for each model: (1) maximum moment at failure, (2) maximum angulation at failure, (3) maximum stress at failure, (4) point of failure, (5) intervertebral disc stress, and (6) influence of adding a C2 pars screw to the multilevel construct.

5. Ethics clearance

Informed written consent was obtained from the volunteer before using CT scans to generate the cervical spine 3D finite element models used in the study. This study did not involve research conducted on human volunteers/animal specimens. No confidential data were collected/published during/after the research from any human participants. Because of the aforementioned reasons, the study was exempted from the need for clearance from the Institutional Ethical Committee.

Results

The intact 3D FE model consisting of the skull base–T1 vertebra was successfully reconstructed through CT and digital image processing utilizing Mimics ver. 10.01 (Materialise), Geomagic Design ver. X16.0 (Geomagic), HyperMesh (Altair Engineering), and ANSYS ver. 18.2. (ANSYS Inc.).

1. Maximum moment at failure

For all models, the load applied was 50 N of compressive force, along with moment variations. The maximum moment generated in the flexion motion at the time of failure was the highest for model 3, i.e., construct with C2 pars + C3–C7 LMS, followed by model 4, i.e., construct with C3–C7 LMS (8 Nm and 5 Nm, respectively). Compared with models 3 and 4, the two models with TPS fixation at C7, i.e., models 1 and 2, elicited a lower maximum moment generated during failure (4 Nm in both models 1 and 2) (Fig. 5).

2. Maximum angulation at failure

In model 1, the maximum moment generated at failure and the maximum angulation in flexion permitted were 4 Nm and 22.5°, respectively. In model 2, the maximum moment generated and the maximum angulation permitted were 4 Nm and 24.4°, respectively. In model 3, the maximum moment generated and the maximum angula-

tion were 8 Nm and 27.8° in flexion, respectively. In model 4, the maximum moment generated and the maximum angulation permitted were 5 Nm and 26.8°, respectively (Fig. 6).

3. Maximum stress at failure

Model 1 tolerated the maximum von Mises stress, whereas model 3 could withstand the least von Mises stress at failure. The maximum von Mises stress tolerated by models 1, 2, 3, and 4 were 939.42 MPa, 938.9 MPa, 917.9 MPa, and 877.4 MPa, respectively.

In model 1, the maximum von Mises stress at the maximum moment at failure at C2 pars screw, C3 LMS, C4 LMS, C5 LMS, C6 LMS, C7 TPS, and rods were 363.3 MPa, 54.1 MPa, 32.8 MPa, 183.4 MPa, 84 MPa, 939.4 MPa, and 419.9 MPa, respectively. In model 2, the maximum von Mises stress at the maximum moment at failure at C3 LMS, C4 LMS, C5 LMS, C6 LMS, C7 TPS, and rods were 243.3 MPa, 153.7 MPa, 174.7 MPa, 78.3 MPa, 938.9 MPa, and 622.6 MPa, respectively. In model 3, the maximum von Mises stress at the maximum moment at failure at the C2 pars screw, C3 LMS, C4 LMS, C5 LMS, C6 LMS, C7 LMS, and rods were 675.1 MPa, 75.9 MPa, 215.5 MPa, 389.8 MPa, 147.7 MPa, 299.9 MPa, and 917.9 MPa, respectively. In model 4, the maximum von Mises stress at the maximum moment at failure at C3 LMS, C4 LMS, C5 LMS, C6 LMS, C7 LMS, and rods were 302.8 MPa, 180.6 MPa, 264.5 MPa, 90.9 MPa, 201.8 MPa, and 877.4 MPa, respectively. The maximum stress generated at the implants during the maximum moment at the time of failure is presented in Table 2.
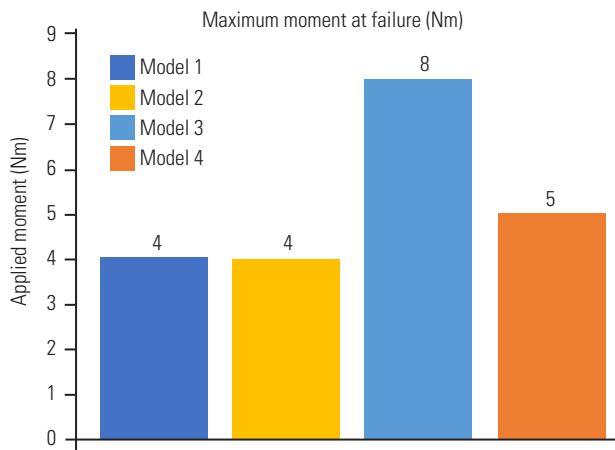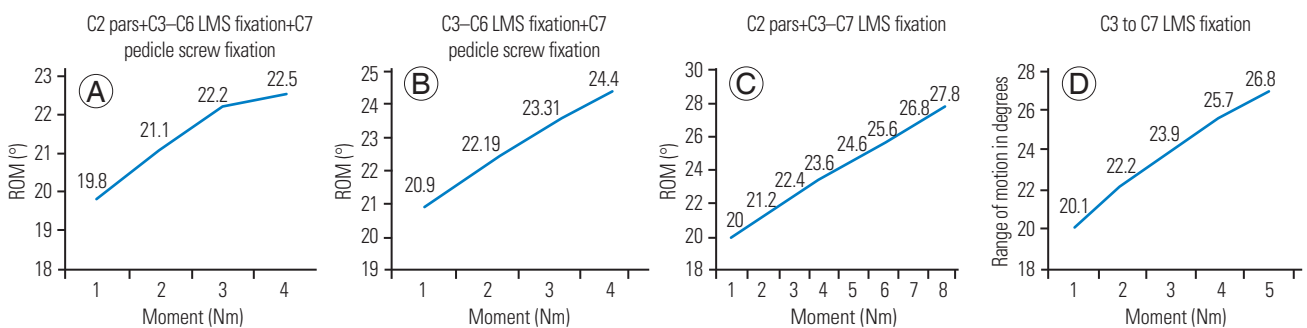

Fig. 5. Maximum moment at failure. The maximum moment generated in the flexion motion at the time of failure was highest for model 3, followed by model 4 (8 Nm and 5 Nm, respectively). Compared to model 3 and 4, the two models with transpedicular screw fixation at C7, i.e., model 1 and model 2, elicited a lower maximum moment generated during failure (4 Nm in both model 1 and 2).

Table 2. Maximum stress at implants at maximum moment in flexion at the time of failure (MPa)

Implant	von Mises stress at flexion a maximum moment on failure (MPa)			
	Model 1	Model 2	Model 3	Model 4
C2 pars screw	363.3	-	675.1	-
C3 LMS	54.1	243.3	75.9	302.8
C4 LMS	132.8	153.7	215.5	180.6
C5 LMS	183.4	174.7	389.8	264.5
C6 LMS	83.0	78.3	147.7	90.9
C7 LMS	-	-	299.9	201.8
C7 TPS	939.4	938.9	-	-
Rods	419.9	622.6	917.9	877.4

LMS, lateral mass screw; TPS, trans-pedicular screw.

Fig. 6. The maximum angulation in flexion with each variation in moment generated is depicted. **(A)** The maximum moment generated at failure in model 1 was 4 Nm and the maximum angulation in flexion permitted was 22.5°. **(B)** The maximum moment generated in model 2 was 4 Nm and the maximum angulation permitted was 24.4°. **(C)** The maximum moment generated in model 3 was 8 Nm and the maximum angulation was 27.8° in flexion. **(D)** The maximum moment generated in model 4 was 5 Nm and the maximum angulation permitted was 26.8°. ROM, range of motion; LMS, lateral mass screw.

4. Point of failure

Models 1 and 2 failed at the C7 TPS at the maximum moment of 4 Nm. Model 3 failed at the C4–C5 rod at the maximum moment of 8 Nm. Model 4 failed at the rod cranially at the C3–C4 level at the maximum moment of 5 Nm (Table 3).

5. Intervertebral disc stress

The intervertebral disc stress (von Mises stress in MPa) at the maximum moment of failure in flexion is provided in Table 4 and Fig. 7. Models 1 and 2 show lesser von Mises stress at C6–C7 and C7–T1 (0.93 MPa and 1.64 MPa, respectively) than model 3 (1.87 MPa and 3.13 MPa, respectively) and model 4 (1.25 MPa and 2.03 MPa, respectively).

6. Influence of adding a C2 pars screw to the multilevel construct

For both models 1 and 3 where C2 fixation was performed, lower von Mises stress was recorded at the C2–C3 intervertebral disc level (Table 4, Fig. 7). Von Mises stress of 1.39 MPa and 2.46 MPa were recorded at C2–C3 in models 1 and 3, respectively. The models as seen on failure, point of failure, trajectory of instruments, and the stress of each component are summarized in the contour plot in Fig. 8.

Discussion

To our knowledge, this is the first study to include FE models to study multilevel posterior cervical fixation constructs and evaluate the biomechanical properties of LMS and TPS at the caudal level, i.e., C7. Existing works include cadaveric and clinical studies comparing the clinicoradiological outcomes of LMS versus TPS at the C7 vertebra [28]. However, these studies have primarily employed monosegmental or bisegmental fixation models. We hope to confirm the validity of existing data with this FE study and use this study as groundwork for future cervical spine FE studies.

The C7 vertebra has a unique anatomy compared with other subaxial vertebrae in terms of its relationship to the vertebral artery and its junctional location in the spinal column [11]. For any multilevel fixation construct, careful planning for the screw fixation at the C7 vertebra is of utmost importance [29]. The distinctive morphology of the lateral masses at the C7 vertebra and its inconsistent relationship to the vertebral artery require careful preoperative planning with appropriate investigative modalities before C7 fixation [30]. Although LMS fixation remains the gold standard for C3–C6 fixation, the ideal choice of the fixation technique at the C7 vertebra in a multilevel posterior cervical fixation construct remains debatable.

Table 3. Point of failure of posterior cervical finite element model

Model	Point of failure
Model 1 (C2 pars+C3–C6 LMS+ C7 TPS)	TPS at C7 vertebra
Model 2 (C3–C6 LMS+C7 TPS)	TPS at C7 vertebra
Model 3 (C2 pars+C3–C7 LMS)	Rod at C4–C5
Model 4 (C3–C7 LMS)	Rod at C3–C4

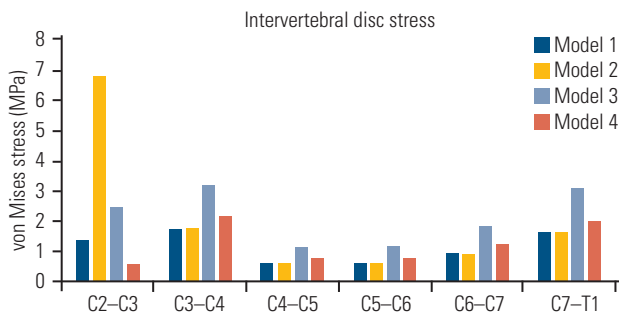LMS, lateral mass screw; TPS, trans-pedicular screw.

Fig. 7. Influence of adding a C2 pars screw to the multi-level construct. For both models where C2 fixation was done, i.e., model 1 and model 3, lower von Mises stress was recorded at the C2–C3 inter-vertebral disc level.

Table 4. Intervertebral disc stress distribution (MPa)

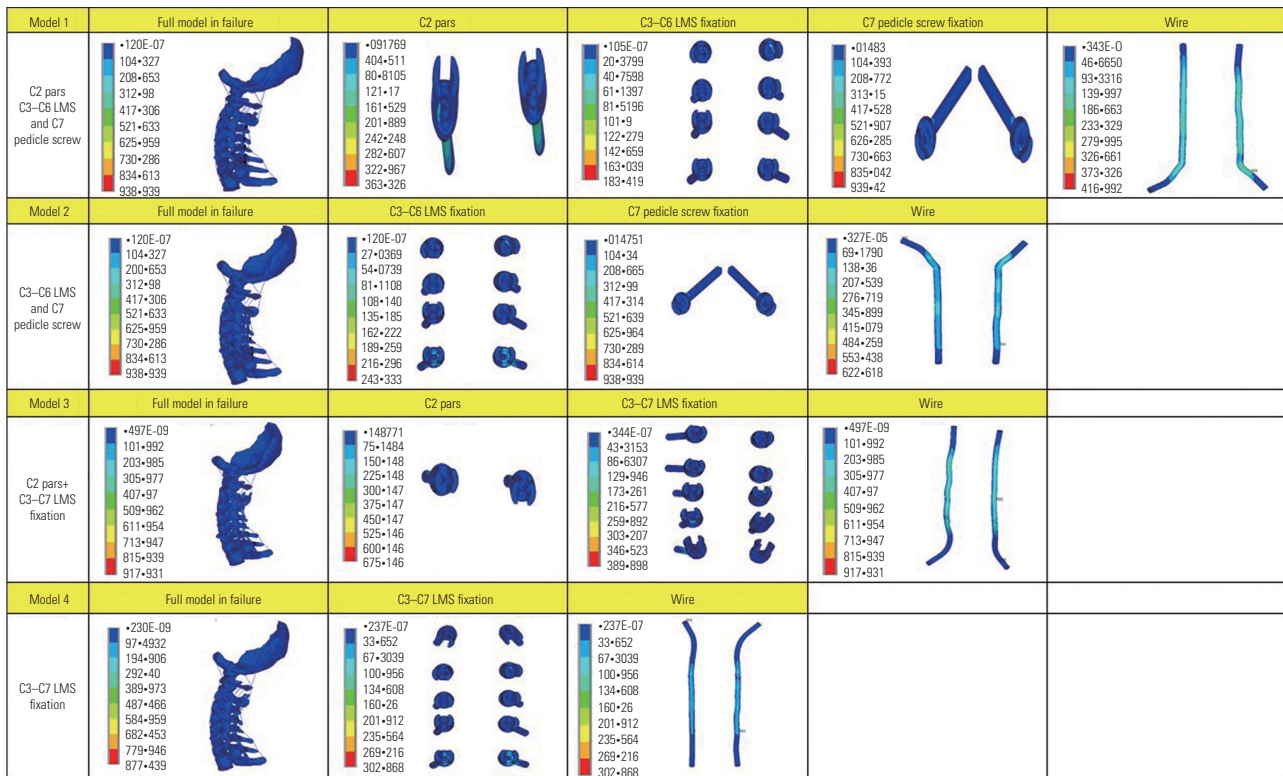| Model	Maximum moment at failure (Nm)	von Mises stress at each intervertebral disc in MPa					
		C2–C3	C3–C4	C4—C5	C5–C6	C6–C7	C7–T1
Model 1	4	1.39	1.73	0.62	0.62	0.93	1.64
Model 2	4	6.86	1.79	0.64	0.63	0.93	1.64
Model 3	8	2.46	3.20	1.15	1.21	1.87	3.13
Model 4	5	0.58	2.18	0.78	0.80	1.25	2.03

Fig. 8. Contour plots depicting the models as seen on failure, the point of failure, the trajectory of instruments and the stress distribution across each component. LMS, lateral mass screw.

LMS and TPS fixations are the two most popular methods of stabilizing the cervical spine. With the combined usage of autogenous bone grafting, LMS fixation in cervical trauma led to fusion rates >95% [31,32]. Because of a smaller lateral mass at the C7 vertebra, LMS fixation at this level often achieves inadequate purchase, thereby requiring TPS fixation of the lower cervical spine and upper thoracic vertebrae. In the past, TPS have greater fixation stability [33-35]. This study was conducted to evaluate differences in the biomechanics of multilevel posterior cervical fixation constructs, ending caudally at the C7 vertebra with LMS and TPS in response to motion and stress.

The maximum moment generated at failure was lower for long subaxial cervical constructs terminating with TPS than those terminating with LMS. The reason was that TPS have a longer lever arm, spanning all three vertebral columns, whereas the LMS anchors only to the posterior column. This in turn provided a stiffer mechanics to the subaxial construct.

The maximum angulation of the cervicothoracic spinal model in flexion was greater for constructs with C7 LMS than those with C7 TPS. This again is attributed to the tricolumnar purchase of TPS fixation compared with LMS fixa-

tion that controls the posterior vertebral column only. These findings are in accordance with the results of Duan et al. [36].

On loading the models with compressive force in flexion motion, the accumulation of von Mises stress over the implants was greater for LMS models than for TPS models. Along with this, the variability in the von Mises stress at each intervertebral disc space was greater for models terminating caudally with LMS than those with TPS. In the analysis of the von Mises stress variability at each intervertebral disc, the concentration of von Mises stress at the implants was considered a measurement of the potential for greater risk of fixation device fracture. In this study, the von Mises stress at C6–C7 and C7–T1 intervertebral discs were lower for TPS than for LMS fixation. This indicated the higher stress shielding nature of the TPS at the C7 vertebra and adjacent disc levels.

For models 1 and 3 where the construct was extending up to C2 fixation proximally, the von Mises stress at the C2–C3 level was lower than that at models 2 and 4 where C2 was unconstrained. The von Mises stress at C2–C3 and C3–C4 was the lowest for model 1 where C2 pars screw and C7 TPS were used. Adding a C2 pars screw to the posterior cervical construct increased the constraint of the

system. It also ensured lesser variability of the von Mises stresses across various levels, thereby reducing the risk of implant fracture and related complications.

The salient features of this study are as follows: (1) This study is the first to include an FE model to evaluate the biomechanics of multilevel posterior cervical fixation with LMS and TPS at the C7 vertebra. (2) Existing literature includes cadaveric and clinical studies comparing the clinicoradiological outcomes of the two fixation modalities. However, these studies have employed monosegmental/bisegmental fixation models. Moreover, clinical studies require a lengthy follow-up. Many patients in these settings are lost by attrition during follow-up.

This study has a few limitations. First, only a one-time fixed compressive force was loaded with flexion angulation. The model was not tested with repetitive stress loading or in extension/side-bending motions. We hope to use this study as the groundwork for more intricate FE studies in the future. Second, the bone–screw contact was modeled as bonded (homogenous entity), ignoring any potential micromotions. The calculated outcomes are solely dependent on simulated conditions and should only be evaluated for reference.

Considering the aforementioned constraints, this study can be a foundation for future research aimed at the dynamic analysis of the subaxial cervical spine construct via multidirectional movements under varied degrees of loading conditions. This study unequivocally validates existing data on multilevel subaxial cervical spine models.

Conclusions

Ending a multilevel cervical construct with TPS fixation rather than LMS fixation at the C7 vertebra provides a stiff and more constrained construct system, with higher stress endurance to compressive force. The constraint and durability of the construct can be further enhanced by adding a C2 pars screw in the fixation system. This study using FEA models provides a platform to study and compare the biomechanical properties of various posterior cervical fixation designs and paves the way for more cervical FE studies in the future.

Conflict of Interest

No potential conflict of interest relevant to this article was reported.

ORCID

Arvind G. Kulkarni: https://orcid.org/0000-0002-0919-7108; Priyambada Kumar: https://orcid.org/0000-0002-7168-4767; Gautam M. Shetty: https://orcid.org/0000-0002-5211-2376; Sandipan Roy: https://orcid.org/0000-0002-6888-272X; Pechimuthu Susai Manickam: https://orcid.org/0000-0001-7507-5726; Raja Dhason: https://orcid.org/0000-0001-6912-697X; Aditya R. S. S. Chadalavada: https://orcid.org/0000-0003-0054-0974; Yogesh M. Adbalwad: https://orcid.org/0009-0003-2475-8609

Author Contributions

Conception and design: AGK, PK, GMS, SR, PSM, RD, YA, AC. Data acquisition: SR, PSM, RD. Data analysis: PK, SR, PSM, RD. Drafting and editing of the manuscript: PK. Critical revision for important intellectual content: AGK. Agree to be accountable for all aspects of the work in ensuring that questions related to the accuracy or integrity of any part of the work are appropriately investigated and resolved: all authors. Final approval of the manuscript: all authors.

References

1. Abumi K, Shono Y, Ito M, Taneichi H, Kotani Y, Kaneda K. Complications of pedicle screw fixation in reconstructive surgery of the cervical spine. Spine (Phila Pa 1976) 2000;25:962-9.

2. Jang WY, Kim IS, Lee HJ, Sung JH, Lee SW, Hong JT. A computed tomography-based anatomic comparison of three different types of c7 posterior fixation techniques: pedicle, intralaminar, and lateral mass screws. J Korean Neurosurg Soc 2011;50:166-72.

3. Kulkarni AG, Dhruv AN, Bassi AJ. Posterior cervicothoracic instrumentation: testing the clinical efficacy of tapered rods (dual-diameter rods). J Spinal Disord Tech 2015;28:382-8.

4. Bozkus H, Ames CP, Chamberlain RH, et al. Biomechanical analysis of rigid stabilization techniques for three-column injury in the lower cervical spine. Spine (Phila Pa 1976) 2005;30:915-22.

5. Schmidt R, Wilke HJ, Claes L, Puhl W, Richter M. Effect of constrained posterior screw and rod systems for primary stability: biomechanical in vitro comparison of various instrumentations in a single-level

corpectomy model. Eur Spine J 2005;14:372-80.

6. Benke MT, O'Brien JR, Turner AW, Yu WD. Biomechanical comparison of transpedicular versus intralaminar C2 fixation in C2-C6 subaxial constructs. Spine (Phila Pa 1976) 2011;36:E33-7.

7. Algarni N, Dea N, Evaniew N, et al. Does ending a posterior construct proximally at C2 versus C3 impact patient reported outcomes in degenerative cervical myelopathy patients up to 24 months after the surgery? Global Spine J 2023 Mar 24 [Epub]. https://doi.org/10.1177/21925682231166605

8. Roy-Camille, R, Saillant GM. Internal fixation of the unstable cervical spine by a posterior osteosynthesis with plates and screws. In: Sherk H, editor. The cervical spine. Philadelphia (PA): Lippincott; 1989. p. 390-403.

9. Yoshihara H, Passias PG, Errico TJ. Screw-related complications in the subaxial cervical spine with the use of lateral mass versus cervical pedicle screws: a systematic review. J Neurosurg Spine 2013;19:614-23.

10. Kwon BK, Vaccaro AR, Grauer JN, Beiner JM. The use of rigid internal fixation in the surgical management of cervical spondylosis. Neurosurgery 2007;60(1 Suppl 1):S118-29.

11. Abumi K, Itoh H, Taneichi H, Kaneda K. Transpedicular screw fixation for traumatic lesions of the middle and lower cervical spine: description of the techniques and preliminary report. J Spinal Disord 1994;7:19-28.

12. Tse MS, Chan CH, Wong KK, Wong WC. Quantitative anatomy of C7 vertebra in southern Chinese for insertion of lateral mass screws and pedicle screws. Asian Spine J 2016;10:705-10.

13. Zhang C, Zhou Q, Arnold PM. Safety and efficacy of lateral mass screws at C7 in the treatment of cervical degenerative disease. Surg Neurol Int 2017;8:218.

14. Mohamed E, Ihab Z, Moaz A, Ayman N, Haitham AE. Lateral mass fixation in subaxial cervical spine: anatomic review. Global Spine J 2012;2:39-46.

15. Xu R, McGirt MJ, Sutter EG, et al. Biomechanical comparison between C-7 lateral mass and pedicle screws in subaxial cervical constructs: presented at the 2009 Joint Spine Meeting: laboratory investigation. J Neurosurg Spine 2010;13:688-94.

16. Biswas JK, Roy S, Pradhan R, Rana M, Majumdar S. Effects of cervical disc replacement and anterior fusion for different bone conditions: a finite element

study. Int J Multiscale Comput Eng 2019;17:411-27.

17. Bhattacharya S, Roy S, Rana M, Banerjee S, Karmakar SK, Biswas JK. Biomechanical performance of a modified design of dynamic cervical implant compared to conventional ball and socket design of an artificial intervertebral disc implant: a finite element study. J Mech Med Biol 2019;19:1950017.

18. Gilad I, Nissan M. A study of vertebra and disc geometric relations of the human cervical and lumbar spine. Spine (Phila Pa 1976) 1986;11:154-7.

19. Manickam PS, Roy S, Shetty GM. Biomechanical evaluation of a novel S-type, dynamic zero-profile cage design for anterior cervical discectomy and fusion with variations in bone graft shape: a finite element analysis. World Neurosurg 2021;154:e199-214.

20. Manickam PS, Ghosh G, Shetty GM, Chowdhury AR, Roy S. Biomechanical analysis of the novel S-type dynamic cage by implementation of teaching learning based optimization algorithm: an experimental and finite element study. Med Eng Phys 2023;112:103955.

21. Manickam PS, Roy S. The biomechanical study of cervical spine: a finite element analysis. Int J Artif Organs 2022;45:89-95.

22. Manickam PS, Roy S. The biomechanical effects of S-type dynamic cage using Ti and PEEK for ACDF surgery on cervical spine varying loads. Int J Artif Organs 2021;44:748-55.

23. Yoganandan N, Kumaresan S, Pintar FA. Geometric and mechanical properties of human cervical spine ligaments. J Biomech Eng 2000;122:623-9.

24. Zhang QH, Teo EC, Ng HW. Development and validation of a CO-C7 FE complex for biomechanical study. J Biomech Eng 2005;127:729-35.

25. Zhang QH, Teo EC, Ng HW, Lee VS. Finite element analysis of moment-rotation relationships for human cervical spine. J Biomech 2006;39:189-93.

26. Wu TK, Meng Y, Wang BY, et al. Biomechanics following skip-level cervical disc arthroplasty versus skip-level cervical discectomy and fusion: a finite element-based study. BMC Musculoskelet Disord 2019;20:49.

27. Arab AZ, Merdji A, Benaissa A, et al. Finite-element analysis of a lateral femoro-tibial impact on the total knee arthroplasty. Comput Methods Programs Biomed 2020;192:105446.

28. Joaquim AF, Mudo ML, Tan LA, Riew KD. Posterior subaxial cervical spine screw fixation: a review of

techniques. Global Spine J 2018;8:751-60.

29. Olguner SK, Arslan A, Acik V, et al. Comparison of two posterior instrumentation techniques in multilevel cervical spondylotic myelopathy treatment: lateral mass screw fixation vs pedicle screw fixation. J Turk Spinal Surg 2021;32:58-64.

30. Abdullah KG, Nowacki AS, Steinmetz MP, Wang JC, Mroz TE. Factors affecting lateral mass screw placement at C-7. J Neurosurg Spine 2011;14:405-11.

31. Stemper BD, Marawar SV, Yoganandan N, Shender BS, Rao RD. Quantitative anatomy of subaxial cervical lateral mass: an analysis of safe screw lengths for Roy-Camille and Magerl techniques. Spine (Phila Pa 1976) 2008;33:893-7.

32. Cooper PR. The Axis Fixation System for posterior instrumentation of the cervical spine. Neurosurgery 1996;39:612-4.

33. Hildingsson C, Jonsson H. Posterior stabilization of the cervical spine with hooks and screws: a clinical evaluation of 26 patients with traumatic, degenerative or metastatic lesions, using a new implant system. Eur Spine J 2001;10:50-4.

34. Ludwig SC, Kramer DL, Balderston RA, Vaccaro AR, Foley KF, Albert TJ. Placement of pedicle screws in the human cadaveric cervical spine: comparative accuracy of three techniques. Spine (Phila Pa 1976) 2000;25:1655-67.

35. Takayasu M, Hara M, Yamauchi K, Yoshida M, Yoshida J. Transarticular screw fixation in the middle and lower cervical spine: technical note. J Neurosurg 2003;99:132-6.

36. Duan Y, Wang HH, Jin AM, et al. Finite element analysis of posterior cervical fixation. Orthop Traumatol Surg Res 2015;101:23-9.